

# RSC Advances



This article can be cited before page numbers have been issued, to do this please use: K. A. Lin and Z. Zhang, *RSC Adv.*, 2016, DOI: 10.1039/C5RA22947B.



This is an *Accepted Manuscript*, which has been through the Royal Society of Chemistry peer review process and has been accepted for publication.

*Accepted Manuscripts* are published online shortly after acceptance, before technical editing, formatting and proof reading. Using this free service, authors can make their results available to the community, in citable form, before we publish the edited article. This *Accepted Manuscript* will be replaced by the edited, formatted and paginated article as soon as this is available.

You can find more information about *Accepted Manuscripts* in the [Information for Authors](#).

Please note that technical editing may introduce minor changes to the text and/or graphics, which may alter content. The journal's standard [Terms & Conditions](#) and the [Ethical guidelines](#) still apply. In no event shall the Royal Society of Chemistry be held responsible for any errors or omissions in this *Accepted Manuscript* or any consequences arising from the use of any information it contains.

# $\alpha$ -Sulfur as a Metal-free Catalyst to Activate Peroxymonosulfate under Visible Light Irradiation for Decolorization

*Kun-Yi Andrew Lin\* and Zhi-Yu Zhang*

Department of Environmental Engineering, National Chung Hsing University,  
250 Kuo-Kuang Road, Taichung, Taiwan, R.O.C.

\*Corresponding Author. Tel: +886-4-22854709, E-mail address: linky@nchu.edu.tw

(Kun-Yi Andrew Lin)

### Abstract

While transition metals have been frequently used to activate peroxymonosulfate (PMS) for chemical oxidation reactions, recently metal-free activation of PMS has also drawn great attention considering that no metal is required and the environmental impact can be minimized. In this study, orthorhombic  $\alpha$ -sulfur ( $\alpha$ -S), as the first time, is employed as a metal-free photocatalyst to activate PMS under visible (Vis) light irradiation. To study the activation of PMS by  $\alpha$ -S/Vis process, decolorization of Rhodamine B (RhB) dye is selected as a model reaction. Parameters affecting the decolorization were investigated, including  $\alpha$ -S loading, PMS dosage, temperature, pH, salt and inhibitors. The decolorization using PMS activated by  $\alpha$ -S/Vis was much faster than the self-activation of PMS. A higher  $\alpha$ -S loading also facilitated the activation of PMS; however, over-loading of  $\alpha$ -S led to the shielding effect, thereby decreasing the decolorization extent. Higher PMS dosages and temperatures were both preferable for the decolorization. While the decolorization was improved under the acidic condition, the activation of PMS was hindered under alkaline conditions. When high concentrations of NaCl were added to RhB solutions, the decolorization extent still remained almost the same. Electron paramagnetic resonance (EPR) spectroscopic analysis was performed to probe into the mechanism of PMS activated by  $\alpha$ -S/Vis process.  $\alpha$ -S/Vis process was found to be recyclable and stable over multiple cycles, even though  $\alpha$ -S did not undergo any regeneration treatments. Considering these features,  $\alpha$ -S/Vis process appears to be a promising and environmentally friendly process to activate PMS for chemical oxidation reactions.

**Keywords:**  $\alpha$ -sulfur, peroxymonosulfate, decolorization, Rhodamine B, visible light

## 1. Introduction

Chemical oxidation reaction is one of the most important reactions, especially in chemical synthesis [1] and contaminant degradation [2-4]. Wet chemical oxidations, like Advanced Oxidation Processes (AOPs) [2, 5-7], typically involve highly reactive oxygenic species such as hydroxyl ( $\text{OH}^\bullet$ ) and sulfate ( $\text{SO}_4^{\bullet-}$ ) radicals [8, 9]. As hydroxyl radical-generated technologies (*e.g.*, Fenton reaction, photo-Fenton, sono-Fenton, electro-Fenton, etc.) have been extensively investigated and developed, sulfate radical-generated processes recently have been also focused considering several advantageous features of sulfate radicals [10] as follows. First, the oxidation potential of  $\text{SO}_4^{\bullet-}$  (2.5–3.1 V vs NHE) is comparable or even higher than that of  $\text{OH}^\bullet$  (2.8 V vs NHE) [11]. Second,  $\text{SO}_4^{\bullet-}$  exhibits a highly selective reactivity toward unsaturated and aromatic electrons [11, 12]. Third, the half-life period of  $\text{SO}_4^{\bullet-}$  (*i.e.*, 30–40  $\mu\text{s}$ ) is much longer than that of  $\text{OH}^\bullet$  (*i.e.*, < 1  $\mu\text{s}$ ) [13, 14].

To obtain sulfate radicals, peroxymonosulfate (PMS) has become an essential source, since it is commercially available and environmental-friendly [10]. Therefore, PMS has been frequently used for bleaching, cleaning, disinfection as well as chemical synthesis [10, 15]. However, PMS must be activated in order to facilitate the generation of sulfate radicals [10, 16-22].

To date, a number of techniques have been used to activate PMS, including metallic catalysts, thermal treatments, and sonication [16-22]. Among these techniques, addition of transition metals (*e.g.*, cobalt oxide [20, 22], iron oxide [20, 23, 24], and manganese oxide [25, 26]) is recognized as a highly efficient approach [20], especially considering that the thermal and ultrasound activation of PMS require continuous and intensive energy input. Nevertheless, in view of the usage of metals, especially noble metals, and the subsequent environmental concerns, non-metal or

metal-free activation of PMS has been focused lately [27]. Sun *et al.* demonstrated using reduced graphene oxide (RGO) to accelerate the activation of PMS [28], since oxygenic species of RGO could initiate the activation. Duan *et al.* further modified RGO with sulfur and nitrogen to improve the activation efficiency of PMS [29, 30]. Tao *et al.* employed a non-metal semiconductor, carbon nitride ( $g\text{-C}_3\text{N}_4$ ), to activate PMS under visible light irradiation [27]. Considering these studies, non-metal and metal-free activation of PMS appears to be a promising and sustainable alternative to activate PMS and it should be further developed.

As ionic sulfur is commonly employed in sulfide photocatalysts and doped in oxide photocatalysts, recently element sulfur is also evaluated as a photocatalyst [31]. Although elemental sulfur has more than 30 allotropes,  $S_8$  is recognized as the most stable configuration under standard pressure and temperature.  $S_8$  can form crystals and comprise three allotropes, including orthorhombic  $\alpha$ -sulfur ( $\alpha$ -S), monoclinic  $\beta$ -sulfur ( $\beta$ -s) and  $\gamma$ -sulfur [31]. Orthorhombic  $\alpha$ -sulfur ( $\alpha$ -S) is considered as the most stable form of elemental sulfur under standard pressure and temperature and it is also confirmed to exhibit visible-light-driven photocatalytic activity [31]. Therefore, it is possible to employ  $\alpha$ -S together with visible light to generate electrons and in turn to activate PMS. Nevertheless, such a metal-free approach, to our best knowledge, has not been explored as a technique to activate PMS. Considering that sulfur is one of the most abundant elements on earth and visible light can be provided from the Sun,  $\alpha$ -S with visible light irradiation ( $\alpha$ -S/Vis) process can be a promising, sustainable and environmental-friendly approach to activate PMS, and therefore must be investigated.

In this study,  $\alpha$ -S was prepared via a wet chemistry method under a mild condition and characterized by scanning electron microscopy (SEM), X-ray diffractometer (XRD) and diffused reflectance spectroscopy (DRS). To examine the

PMS activation by  $\alpha$ -S/Vis process, decolorization of Rhodamine B (RhB) dye was selected as a model reaction. Parameters influencing the decolorization using PMS activated by  $\alpha$ -S/Vis process were examined, including  $\alpha$ -S loading, PMS dosage, temperature, pH, salt as well as inhibitive scavengers. To probe in the mechanism of PMS activated by  $\alpha$ -S/Vis, Electron paramagnetic resonance (EPR) spectroscopic analysis was performed. The recyclability of  $\alpha$ -S without regeneration treatment was also evaluated by testing  $\alpha$ -S/Vis for the decolorization over 10 cycles.

## 2. Experimental

### 2.1 Synthesis and characterization of $\alpha$ -S

The orthorhombic  $\alpha$ -sulfur ( $\alpha$ -S) crystal was synthesized according to a reported procedure [32]. In brief, 3 g of  $\text{Na}_2\text{S}_2\text{O}_3$  (Sigma-Aldrich, USA) was dissolved in 0.5 L of DI water, followed by an addition of 6 ml of Triton TX-100 (Sigma-Aldrich, USA) aqueous solution (1 wt%) at 50 °C. The mixture was then heated to 70 °C and 24 ml of concentrated HCl aqueous solution was added to the mixture, which was stirred for 5hr. The precipitate was collected via centrifugation, washed thoroughly with DI water and dried at 65 °C for 12 hr to obtain the yellowish powder,  $\alpha$ -S.

Physical and chemical characteristics of the as-prepared  $\alpha$ -S powder were determined first by a field emission SEM (JEOL JSM-6700, Japan) to visualize its morphology. The XRD pattern of  $\alpha$ -S was obtained using an X-ray diffractometer with copper as an anode material (40 mA, 45 kV) (PANalytical, the Netherlands). DRS measurement of  $\alpha$ -S was performed using a UV-Vis spectrophotometer equipped with integrating spheres (Jasco V650, Japan).

### 2.2 Dye decolorization using PMS activated by $\alpha$ -S/Vis process

Decolorization of RhB dye in water was conducted as a model test to evaluate the activation of PMS and it was performed in a batch reactor as follows. First, 0.1 g of  $\alpha$ -S was dispersed in a 0.2 L of RhB aqueous solution with an initial concentration ( $C_0$ ) of 10 mg L<sup>-1</sup>. Subsequently, 0.06 g of PMS powder (Sigma-Aldrich, USA) was immediately added to the RhB solution which was irradiated by visible light lamp (150W Philips, Netherland) with UV light cut-off. The light intensity irradiating the reactor was  $110 \times 10^3$  Lux (equivalent to 0.016 watt cm<sup>-2</sup>) measured by a light meter (TES 1335, China). The batch reactor was equipped with a water-circulation system to maintain solution temperatures. At pre-set times, sample aliquots were withdrawn from the batch reactor and the remaining RhB concentration ( $C_t$ , mg L<sup>-1</sup>) was analyzed by a UV-Vis spectrophotometer (e-ChomTech CT-2000, Taiwan).

To evaluate effects of catalyst loading and oxidant dosage, the addition of  $\alpha$ -S was varied from 250 to 1500 mg L<sup>-1</sup>. PMS dosage was also changed from 100 to 300 mg L<sup>-1</sup>. The decolorization test was conducted at different temperatures to study the effect of temperature and to determine the activation energy ( $E_a$ ) of the activation of PMS by  $\alpha$ -S/Vis process. Effects of pH and salt on the RhB decolorization were also evaluated. pH values were changed to 3, 7, 9 and 11 to investigate the decolorization under acidic, neutral, weakly basic and basic conditions, respectively. The effect of salt was evaluated by adding different amounts of NaCl (*i.e.*, 1000, 1500 and 2000 mg L<sup>-1</sup>) to RhB solutions. Several inhibitors were also added to RhB solutions during the decolorization to evaluate their inhibitive effects and to provide insights into the activation mechanism. The inhibitors included ascorbic acid (0.01 M), methanol (0.2 M) and *tert*-butyl alcohol (TBA) (0.2 M). Since the inhibitive effect of ascorbic acid was significantly stronger than methanol and TBA, the dosage of ascorbic acid was much less than that of methanol as well as TBA. To further probe into the mechanism,

EPR spectroscopy was employed using 5,5-Dimethyl-1-pyrroline N-oxide (DMPO) as a radical-trapping agent. EPR spectra of PMS activated by  $\alpha$ -S with and without the visible light irradiation were measured by Bruker EPR spectrometer (EMX-P, Germany). To examine the recyclability of  $\alpha$ -S/Vis process to activate PMS,  $\alpha$ -S was re-used for 10 cycles without any regeneration treatments.

### 3. Results and Discussion

#### 3.1 Characterization of $\alpha$ -S

A macroscopic view of  $\alpha$ -S is shown on the right side of Fig. 1(a). One can see that  $\alpha$ -S crystals are fine yellowish powder. The chemical structure of  $\alpha$ -S is typically represented as a ring-like structure from the top view (Fig. 1(b)) and a crown-like structure from the side view (Fig. 1(c)). The morphology of  $\alpha$ -S crystals is further revealed in detail in Fig. 2(a).  $\alpha$ -S particles were irregular and the size of  $\alpha$ -S particles was around 5 micrometers. A closer view of  $\alpha$ -S (Fig. S1, see ESI†) shows that  $\alpha$ -S exhibited surface roughness and no obvious porosity was observed. The crystalline structure of  $\alpha$ -S is revealed in Fig. 2(b) and its XRD pattern can be readily indexed for the orthorhombic sulfur (JCPDS Standard 08-0247) [33], confirming the formation of  $\alpha$ -S crystals. The optical absorption property of  $\alpha$ -S is shown in Fig. 2(c), which displays an onset of adsorption of  $\alpha$ -S at 500 nm as reported in a previous literature [31]. The experimental band gap of  $\alpha$ -S has been determined to be 2.79 eV [31].

#### 3.2 Decolorization using PMS activated by $\alpha$ -S under visible light irradiation

Since the RhB dye might be decolorized by  $\alpha$ -S via adsorption, we first evaluated the adsorption of RhB to  $\alpha$ -S in Fig. 3. It can be seen that no RhB was decolorized through the adsorption to  $\alpha$ -S, indicating that there was no strong affinity between  $\alpha$ -S

and RhB. Furthermore, the decolorization by  $\alpha$ -S under visible light irradiation was also evaluated (Fig. 3). Unlike the adsorption to  $\alpha$ -S, RhB was slightly decolorized by the photocatalysis of  $\alpha$ -S. This was possibly because  $\alpha$ -S under the visible light irradiation resulted in electrons which subsequently became certain reactive oxygenic species (*e.g.*,  $\text{OH}^\bullet$ ) to degrade RhB. Furthermore, the RhB decolorization using PMS alone (under visible light irradiation) was examined as a reference for comparison with PMS activated by  $\alpha$ -S/Vis process. Even though PMS itself was able to decolorize RhB (Fig. 3),  $C_t/C_0$  only approached  $\sim 0.35$  in 100 min, indicating that the activation of PMS without catalysts was quite slow. Nevertheless, when PMS was added to the RhB solution in the presences of  $\alpha$ -S and visible light irradiation, the kinetics of the RhB decolorization became significantly faster and  $C_t/C_0$  reached zero in 50 min. UV-visible spectroscopic analysis (Fig. S2, see **ESI†**) also shows that RhB dye diminished along the reaction time. This suggests that the activation of PMS in the presences of  $\alpha$ -S and visible light irradiation was remarkably accelerated. In order to determine the enhancement in the decolorization using  $\alpha$ -S/Vis process, the decolorization kinetics was analyzed using the pseudo first order rate law (Eq. (1)):

$$C_t = C_0 \exp(-k_1 t) \quad (1)$$

where  $k_1$  is the first order rate constant of the decolorization. The  $k_1$  values of PMS alone and PMS activated by  $\alpha$ -S/Vis were calculated and listed in Table 1. When PMS alone was used,  $k_1$  was  $0.008 \text{ min}^{-1}$ . After  $\alpha$ -S was added to the solution,  $k_1$  became  $0.064 \text{ min}^{-1}$ . This comparison validates that  $\alpha$ -S together with visible light irradiation was able to activate PMS for the generation of sulfate radicals.

### 3.3 Effects of $\alpha$ -S loading and PMS dosage on the decolorization

To further investigate the roles of  $\alpha$ -S and PMS in the PMS activation for the decolorization,  $\alpha$ -S loadings and PMS dosages were varied to study their respective effects. Fig. 4(a) shows the decolorization using different  $\alpha$ -S loadings. When  $\alpha$ -S loading was 250 mg L<sup>-1</sup>, the decolorization proceeded quite slowly and  $C_t/C_0$  did not reach 0 even after 100 min. Once  $\alpha$ -S loading became 500 mg L<sup>-1</sup>, the decolorization kinetics became faster and  $C_t/C_0$  approached 0 in 50 min. To quantitatively compare the kinetics using different  $\alpha$ -S loadings, the pseudo first order rate law was employed.  $k_1$  for  $\alpha$ -S loading = 250 mg L<sup>-1</sup> was 0.022 min<sup>-1</sup>, whereas  $k_1$  was 0.064 min<sup>-1</sup> in the case of  $\alpha$ -S loading = 500 mg L<sup>-1</sup>, indicating that  $\alpha$ -S loading can affect the activation of PMS. When  $\alpha$ -S loading was increased to 1000 mg L<sup>-1</sup>, the decolorization kinetics ( $k_1 = 0.0534$  min<sup>-1</sup>) and efficiency, however, did not improve significantly. Interestingly, as  $\alpha$ -S loading was further raised to 1500 mg L<sup>-1</sup>, the decolorization kinetics ( $k_1 = 0.0344$  min<sup>-1</sup>) and efficiency became slower and lower, respectively. This result suggests that even though a higher  $\alpha$ -S loading facilitated the PMS activation, over-loading of  $\alpha$ -S might lead to adverse effects. This could be due to that  $\alpha$ -S particles suspending in the solution blocked the visible light irradiation and the shielding effect decreased the catalytic activity of  $\alpha$ -S for the activation of PMS.

The effect of PMS dosage was evaluated in Fig. 4(b), in which the PMS dosage was changed from 100 to 400 mg L<sup>-1</sup>. An obvious trend can be observed that a lower PMS dosage led to the slower decolorization kinetics, whereas a higher PMS dosage improved the decolorization. The decolorization was also decreased with a lower PMS dosage as  $C_t/C_0$  did not reach 0 even after 100 min with PMS dosage of 100 and 200 mg L<sup>-1</sup>. The corresponding  $k_1$  values are summarized in Table 1. When PMS dosage changed from 100 to 200, 300 and 400 mg L<sup>-1</sup>,  $k_1$  increased from 0.010, 0.016,

0.064 and then 0.094 min<sup>-1</sup>. Although the decolorization kinetics was indeed faster using PMS of 400 mg L<sup>-1</sup>, the improvement in kinetics from PMS of 300 to 400 mg L<sup>-1</sup> was not as significant as that from 200 to 300 mg L<sup>-1</sup>. Nevertheless, the higher PMS dosage leads to a higher amount of PMS consumption, increasing operation cost. Therefore, an optimal PMS dosage has to be traded off between decolorization performance and operation cost.

### 3.4 Effects of temperature and pH on the RhB decolorization

Additionally, the effect of temperature on the decolorization was also studied in Fig. 5(a). When temperature was changed from 40 to 20 °C, RhB dye was still fully decolorized after 100 min. Nevertheless, the kinetics became much slower as  $k_I$  decreased from 0.064 to 0.025 min<sup>-1</sup>. In contrast, as the temperature varied from 40 to 60 °C, the decolorization kinetics was improved significantly and  $C_t/C_0$  approached 0 within 20 min. The rate constant ( $k_I$ ) at 60 °C was 0.143 min<sup>-1</sup>, much higher than  $k_I$  obtained at 40 °C. This suggests that the activation of PMS by  $\alpha$ -S/Vis process can be greatly facilitated at a higher temperature as reported in literatures [19].

The rate constants ( $k_I$ ) at different temperatures can be further analyzed using the Arrhenius equation to determine the activation energy ( $E_a$ , kJ mol<sup>-1</sup>) of PMS activated by  $\alpha$ -S/Vis process using the following equation (Eq.(2)):

$$\ln k_I = \ln k - E_a/RT \quad (2)$$

where  $k$  represents the temperature-independent factor (g mg<sup>-1</sup> min<sup>-1</sup>);  $R$  is the universal gas constant;  $T$  is the solution temperature in Kelvin (K). A plot of  $1/T$  versus  $\ln k_I$  is shown in Fig. S3 (see ESI†), in which the data points are perfectly fitted by the linear regression with  $R^2 = 0.999$ . This indicates that the kinetics of the

decolorization using PMS activated by  $\alpha$ -S/Vis process can be well correlated to temperature using the Arrhenius equation. According to the slope and intercept of the linear plot in Fig. S3, the  $E_a$  and  $k$  were determined to be 35.2 kJ mol<sup>-1</sup> and 47.5 mg<sup>-1</sup> min<sup>-1</sup>, respectively.

Furthermore, pH of RhB solution was also varied to investigate the effect of pH. Fig. 5(b) shows the RhB decolorization at pH = 3, 7, 9 and 11, and there was a notable trend that the decolorization and the kinetics became lower and slower, respectively, as pH increased. When pH was adjusted to 3, the RhB was fully decolorized within a very short time (*i.e.*, 10 min).  $k_I$  was found to be 0.522 min<sup>-1</sup> (Table 1), which was much higher than  $k_I$  obtained at the unadjusted pH (*i.e.*, 3.7). Nevertheless, at pH = 7, even though RhB was still fully decolorized, the decolorization kinetics became much slower with  $k_I = 0.048$  min<sup>-1</sup>. Once pH was further raised to 9 and 11, the adverse effect of alkaline condition became even more obvious.  $k_I$  values were found to be 0.024 and 0.005 min<sup>-1</sup> for the decolorization tests at pH = 9 and 11, respectively. These results suggest that PMS activated by  $\alpha$ -S/Vis process is more favorable under acidic conditions, possibly because PMS is relatively stable at low pH [34]. On the other hand, the alkaline conditions might lead to the self-decomposition of PMS without formation of sulfate radicals [34-36] and consequently decreased the decolorization extent.

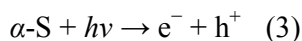
### 3.5 Effects of salt and inhibitors and the proposed mechanism

Considering that dye-containing wastewater may contain other compounds, especially salts, we also investigated the effect of NaCl as a typical salt. By varying NaCl concentration, the effect of ionic strength on the PMS activation was also examined. Fig. 6(a) shows the RhB decolorization with different concentrations of NaCl. Compared to the test without NaCl, the presence of NaCl did not cause substantial changes on the decolorization. The decolorization tests with NaCl = 1000 and 1500 mg L<sup>-1</sup> remained almost the same to the test without NaCl. Although the decolorization kinetics appeared to be slower when NaCl was 2000 mg L<sup>-1</sup>, the change was not significant, indicating that the activation of PMS by  $\alpha$ -S/Vis process was quite stable even with a high concentration of salt.

Besides, we also evaluated the effects of several inhibitors which might scavenge radical species and hinder the decolorization. Through the examination of particular inhibitors, the mechanism of PMS activated by  $\alpha$ -S/Vis process might also be revealed. As shown in Fig. 6(b), when ascorbic acid was added to RhB solutions, the decolorization extent and kinetics both decreased. This was because ascorbic acid is considered as a universal radical scavenger which considerably hindered the generation of sulfate radicals. This also reveals the crucial role of radicals in this radical-driven decolorization reaction. Subsequently, another inhibitor, *tert*-butyl alcohol (TBA), was added to RhB solutions and TBA has been recognized as a probe reagent specifically for hydroxyl radicals. As revealed in Fig. 6(b), the decolorization extent and kinetics were indeed decreased, suggesting that the RhB decolorization using PMS activated by  $\alpha$ -S/Vis process partially involved hydroxyl radicals. On the other hand, methanol was also added to RhB solutions as it is a probe reagent for both hydroxyl and sulfate radicals. In the presence of methanol, the decolorization extent

and kinetics both were significantly decreased. This reveals that the activation of PMS by  $\alpha$ -S/Vis process certainly involved with hydroxyl and sulfate radicals.

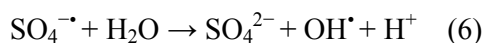
Considering the semiconducting property of  $\alpha$ -S, the visible light irradiation on  $\alpha$ -S can lead to generation of electrons ( $e^-$ ) and holes ( $h^+$ ) as follows (Eq.(3)):



The resultant electrons and holes may react with PMS to form sulfate radicals as follows (Eqs.(4)-(5)) [37]:



The result sulfate radical (*i.e.*,  $\text{SO}_4^{\cdot-}$ ) might react with  $\text{H}_2\text{O}$  to generate the hydroxyl radical (*i.e.*,  $\text{OH}^{\cdot}$ ) as follows (Eq. (6))[38]:



Both sulfate radicals (*i.e.*, 2.5–3.1 V) and hydroxyl radicals (*i.e.*, 2.8 V) possess high oxidizing powers to attack chromophoric groups of dye and cause the decolorization. Based on the above-mentioned possible reaction routes, the EPR analysis was also performed to observe occurrence of radical species during the activation of PMS by  $\alpha$ -S/Vis process. We first measured EPR spectra of a mixture of  $\alpha$ -S and DMPO with and without the visible light irradiation (Fig. 7). When the light was off, no significant peaks were observed. However, once the visible light was introduced, several peaks can be observed, corresponding to occurrence of hydroxyl radicals. This validates that  $\alpha$ -S exhibited photocatalytic activity and utilized photons to generate electrons which reacted with water to form hydroxyl radicals. On the other hand, we also measured EPR spectra of mixtures of  $\alpha$ -S, PMS and DMPO with and without visible light irradiation. In the absence of visible light irradiation, almost no peak was observed from the spectrum, indicating that no noticeable amount of

radicals generated when  $\alpha$ -S was mixed with PMS. This suggests that  $\alpha$ -S alone was ineffective to accelerate the PMS activation. In contrast, when the visible light irradiation was given, a number of peaks appeared and these peaks were identified as occurrences of sulfate radicals as well as hydroxyl radicals [30, 39]. This result indicates that  $\alpha$ -S together with visible light irradiation considerably accelerated the PMS activation, leading to generation of sulfate radicals and subsequently hydroxyl radicals. Based on the result of the effect of inhibitors and the above-mentioned EPR analysis, a proposed mechanism is also schematically presented in Fig. 8.

### 3.6 Multiple-cycle of $\alpha$ -S/Vis process for the RhB decolorization

Since  $\alpha$ -S was proposed as a catalyst to activate PMS, it is critical to examine its recyclability and stability. To evaluate the recyclability of  $\alpha$ -S, the used  $\alpha$ -S powder was recovered from a previous experiment and added to a subsequent test without any regeneration treatments. Fig. 9 shows the decolorization efficiencies (defined as  $(1-C_t/C_0)$  %) over 10 cycles using  $\alpha$ -S/Vis process and the decolorization efficiency remained almost the same during the 10 cycles. The pseudo first order rate constants ( $k_t$ ) of the multi-cycle test are also determined and shown in Fig. 9. While slight variation in  $k_t$  can be noticed,  $k_t$  still remains quite comparable over 10 cycles. These results reveal that  $\alpha$ -S can be a stable and recyclable catalyst to facilitate the activation of PMS under the visible light irradiation. Thus,  $\alpha$ -S/Vis process can be considered as a sustainable and environmentally friendly process for the PMS activation, which is employed in wastewater treatment and chemical synthesis considering that no metal is required and solar light can be a renewable energy input.

#### 4. Conclusion

In this study,  $\alpha$ -S, as the first time, was used as a metal-free photocatalyst to activate PMS under visible light irradiation. Through RhB decolorization, the activation of PMS by  $\alpha$ -S/Vis process was successfully demonstrated. The decolorization using PMS activated by  $\alpha$ -S/Vis was much faster than the self-activation of PMS. A higher  $\alpha$ -S loading was found to facilitate the PMS decomposition while over-loading of  $\alpha$ -S led to the shielding effect which blocked the visible light, thereby decreasing the RhB decolorization. A higher PMS dosage and a higher temperature were both preferable for the activation of PMS for the decolorization. While the acidic condition improved the RhB decolorization, the activation of PMS was greatly hindered under alkaline conditions. Nevertheless, the RhB decolorization remained almost the same even though high concentrations of NaCl were added to RhB solutions. The mechanism of PMS activated by  $\alpha$ -S/Vis process might be attributed to the generation of sulfate radicals derived from the reaction between the resultant electrons of  $\alpha$ -S/Vis process and PMS. Such a process was also found to be recyclable and stable over multiple cycles even though  $\alpha$ -S did not undergo any regeneration treatments. Considering these features,  $\alpha$ -S/Vis process can be employed as a sustainable and environmentally friendly process for the PMS activation as no metal is required and visible light can be obtained from a renewable energy input, the Sun.

**References:**

- [1] W.F. Hoelderich, F. Kollmer, Oxidation reactions in the synthesis of fine and intermediate chemicals using environmentally benign oxidants and the right reactor system, *Pure Appl. Chem.*, 72 (2000) 1273-1287.
- [2] M.A. Oturan, J.-J. Aaron, Advanced Oxidation Processes in Water/Wastewater Treatment: Principles and Applications. A Review, *Critical Reviews in Environmental Science and Technology*, 44 (2014) 2577-2641.
- [3] K. Ikehata, N. Jodeiri Naghashkar, M. Gamal El-Din, Degradation of Aqueous Pharmaceuticals by Ozonation and Advanced Oxidation Processes: A Review, *Ozone: Science & Engineering*, 28 (2006) 353-414.
- [4] M. Klavarioti, D. Mantzavinos, D. Kassinos, Removal of residual pharmaceuticals from aqueous systems by advanced oxidation processes, *Environment International*, 35 (2009) 402-417.
- [5] R. Munter, Advanced Oxidation Processes – Current Status And Prospects, *Proc. Estonian Acad. Sci. Chem*, 50 (2001) 59–80.
- [6] G. Ruppert, R. Bauer, G. Heisler, UV-O<sub>3</sub>, UV-H<sub>2</sub>O<sub>2</sub>, UV-TiO<sub>2</sub> and the photo-Fenton reaction - comparison of advanced oxidation processes for wastewater treatment, *Chemosphere*, 28 (1994) 1447-1454.
- [7] R. Andreozzi, V. Caprio, A. Insola, R. Marotta, Advanced oxidation processes (AOP) for water purification and recovery, *Catalysis Today*, 53 (1999) 51-59.
- [8] W.H. Glaze, J.W. Kang, Advanced oxidation processes. Description of a kinetic model for the oxidation of hazardous materials in aqueous media with ozone and hydrogen peroxide in a semibatch reactor, *Industrial & Engineering Chemistry Research*, 28 (1989) 1573-1580.
- [9] A. Tsitonaki, B. Petri, M. Crimi, H. Mosbæk, R.L. Siegrist, P.L. Bjerg, In Situ Chemical Oxidation of Contaminated Soil and Groundwater Using Persulfate: A Review, *Critical Reviews in Environmental Science and Technology*, 40 (2010) 55-91.
- [10] P. Hu, M. Long, Cobalt-catalyzed sulfate radical-based advanced oxidation: A review on heterogeneous catalysts and applications, *Applied Catalysis B: Environmental*, 181 (2016) 103-117.
- [11] P. Neta, R.E. Huie, A.B. Ross, Rate Constants for Reactions of Inorganic Radicals in Aqueous Solution, *Journal of Physical and Chemical Reference Data*, 17 (1988) 1027-1284.
- [12] M.G. Antoniou, A.A. de la Cruz, D.D. Dionysiou, Degradation of microcystin-LR using sulfate radicals generated through photolysis, thermolysis and e<sup>-</sup> transfer mechanisms, *Applied Catalysis B: Environmental*, 96 (2010) 290-298.

- [13] T. Olmez-Hanci, I. Arslan-Alaton, Comparison of sulfate and hydroxyl radical based advanced oxidation of phenol, *Chem. Eng. J.*, 224 (2013) 10-16.
- [14] E.G. Janzen, Y. Kotake, H. Randall D, Stabilities of hydroxyl radical spin adducts of PBN-type spin traps, *Free Radical Biology and Medicine*, 12 (1992) 169-173.
- [15] P.J. Harrington, *Pharmaceutical Process Chemistry for Synthesis: Rethinking the Routes to Scale-Up*, John Wiley & Sons, Hoboken, New Jersey, 2011.
- [16] G.P. Anipsitakis, E. Stathatos, D.D. Dionysiou, Heterogeneous Activation of Oxone Using  $\text{Co}_3\text{O}_4$ , *The Journal of Physical Chemistry B*, 109 (2005) 13052-13055.
- [17] G. Wei, X. Liang, Z. He, Y. Liao, Z. Xie, P. Liu, S. Ji, H. He, D. Li, J. Zhang, Heterogeneous activation of Oxone by substituted magnetites  $\text{Fe}_3\text{-xMxO}_4$  (Cr, Mn, Co, Ni) for degradation of Acid Orange II at neutral pH, *Journal of Molecular Catalysis A: Chemical*, 398 (2015) 86-94.
- [18] L. Hu, F. Yang, W. Lu, Y. Hao, H. Yuan, Heterogeneous activation of oxone with  $\text{CoMg/SBA-15}$  for the degradation of dye Rhodamine B in aqueous solution, *Applied Catalysis B: Environmental*, 134–135 (2013) 7-18.
- [19] K.-Y.A. Lin, H.-A. Chang, R.-C. Chen, MOF-derived magnetic carbonaceous nanocomposite as a heterogeneous catalyst to activate oxone for decolorization of Rhodamine B in water, *Chemosphere*, 130 (2015) 66-72.
- [20] Q. Yang, H. Choi, S.R. Al-Abed, D.D. Dionysiou, Iron–cobalt mixed oxide nanocatalysts: Heterogeneous peroxymonosulfate activation, cobalt leaching, and ferromagnetic properties for environmental applications, *Applied Catalysis B: Environmental*, 88 (2009) 462-469.
- [21] S. Yang, P. Wang, X. Yang, L. Shan, W. Zhang, X. Shao, R. Niu, Degradation efficiencies of azo dye Acid Orange 7 by the interaction of heat, UV and anions with common oxidants: Persulfate, peroxymonosulfate and hydrogen peroxide, *Journal of Hazardous Materials*, 179 (2010) 552-558.
- [22] C. Cai, H. Zhang, X. Zhong, L. Hou, Ultrasound enhanced heterogeneous activation of peroxymonosulfate by a bimetallic  $\text{Fe-Co/SBA-15}$  catalyst for the degradation of Orange II in water, *J Hazard. Mater.*, 283 (2015) 70-79.
- [23] F. Gong, L. Wang, D. Li, F. Zhou, Y. Yao, W. Lu, S. Huang, W. Chen, An effective heterogeneous iron-based catalyst to activate peroxymonosulfate for organic contaminants removal, *Chem. Eng. J.*, 267 (2015) 102-110.
- [24] J. Zou, J. Ma, L. Chen, X. Li, Y. Guan, P. Xie, C. Pan, Rapid Acceleration of Ferrous Iron/Peroxymonosulfate Oxidation of Organic Pollutants by Promoting  $\text{Fe(III)/Fe(II)}$  Cycle with Hydroxylamine, *Environmental Science & Technology*, 47 (2013) 11685-11691.

- [25] E. Saputra, S. Muhammad, H. Sun, H.-M. Ang, M.O. Tadé, S. Wang, Manganese oxides at different oxidation states for heterogeneous activation of peroxymonosulfate for phenol degradation in aqueous solutions, *Applied Catalysis B: Environmental*, 142–143 (2013) 729-735.
- [26] E. Saputra, S. Muhammad, H. Sun, A. Patel, P. Shukla, Z.H. Zhu, S. Wang,  $\alpha$ -MnO<sub>2</sub> activation of peroxymonosulfate for catalytic phenol degradation in aqueous solutions, *Catalysis Communications*, 26 (2012) 144-148.
- [27] Y. Tao, Q. Ni, M. Wei, D. Xia, X. Li, A. Xu, Metal-free activation of peroxymonosulfate by g-C<sub>3</sub>N<sub>4</sub> under visible light irradiation for the degradation of organic dyes, *RSC Adv.*, 5 (2015) 44128-44136.
- [28] H. Sun, S. Liu, G. Zhou, H.M. Ang, M.O. Tadé, S. Wang, Reduced Graphene Oxide for Catalytic Oxidation of Aqueous Organic Pollutants, *ACS Applied Materials & Interfaces*, 4 (2012) 5466-5471.
- [29] X. Duan, K. O'Donnell, H. Sun, Y. Wang, S. Wang, Sulfur and Nitrogen Co-Doped Graphene for Metal-Free Catalytic Oxidation Reactions, *Small*, (2015) n/a-n/a.
- [30] X. Duan, Z. Ao, H. Sun, S. Indrawirawan, Y. Wang, J. Kang, F. Liang, Z.H. Zhu, S. Wang, Nitrogen-Doped Graphene for Generation and Evolution of Reactive Radicals by Metal-Free Catalysis, *ACS Applied Materials & Interfaces*, 7 (2015) 4169-4178.
- [31] G. Liu, P. Niu, L. Yin, H.-M. Cheng,  $\alpha$ -Sulfur Crystals as a Visible-Light-Active Photocatalyst, *Journal of the American Chemical Society*, 134 (2012) 9070-9073.
- [32] W. Wang, J.C. Yu, D. Xia, P.K. Wong, Y. Li, Graphene and g-C<sub>3</sub>N<sub>4</sub> Nanosheets Cowrapped Elemental  $\alpha$ -Sulfur As a Novel Metal-Free Heterojunction Photocatalyst for Bacterial Inactivation under Visible-Light, *Environmental Science & Technology*, 47 (2013) 8724-8732.
- [33] L.G. Devi, M.L. ArunaKumari, Synergistic effect between orthorhombic  $\alpha$ -Sulfur and TiO<sub>2</sub> as co-photocatalysts for efficient degradation of methylene blue: A mechanistic approach, *J. Mol. Catal. A-Chem.*, 391 (2014) 99-104.
- [34] W. Guo, S. Su, C. Yi, Z. Ma, Degradation of antibiotics amoxicillin by Co<sub>3</sub>O<sub>4</sub>-catalyzed peroxymonosulfate system, *Environmental Progress & Sustainable Energy*, 32 (2013) 193-197.
- [35] A. Rastogi, S.R. Al-Abed, D.D. Dionysiou, Sulfate radical-based ferrous-peroxymonosulfate oxidative system for PCBs degradation in aqueous and sediment systems, *Applied Catalysis B: Environmental*, 85 (2009) 171-179.
- [36] J. Sun, X. Li, J. Feng, X. Tian, Oxone/Co<sup>2+</sup> oxidation as an advanced oxidation process: Comparison with traditional Fenton oxidation for treatment of landfill leachate, *Water Research*, 43 (2009) 4363-4369.

- [37] X. Chen, W. Wang, H. Xiao, C. Hong, F. Zhu, Y. Yao, Z. Xue, Accelerated TiO<sub>2</sub> photocatalytic degradation of Acid Orange 7 under visible light mediated by peroxymonosulfate, *Chemical Engineering Journal*, 193–194 (2012) 290-295.
- [38] L.J. Xu, W. Chu, L. Gan, Environmental application of graphene-based CoFe<sub>2</sub>O<sub>4</sub> as an activator of peroxymonosulfate for the degradation of a plasticizer, *Chem. Eng. J.*, 263 (2015) 435-443.
- [39] S. Indrawirawan, H. Sun, X. Duan, S. Wang, Low temperature combustion synthesis of nitrogen-doped graphene for metal-free catalytic oxidation, *J. Mater. Chem. A*, 3 (2015) 3432-3440.

Table 1 The kinetic parameters derived from the pseudo first order rate law for the decolorization using  $\alpha$ -S with visible light irradiation ( $\alpha$ -S/Vis) under various conditions.

Conditions				The pseudo first order rate law	
$\alpha$ -S	PMS	Temp. (°C)	pH	$k_1$ (min <sup>-1</sup> )	$R^2$
0	300	40	3.7	0.008	0.984
500	300	40	3.7	0.064	0.950
250	300	40	3.7	0.022	0.972
1000	300	40	3.7	0.053	0.970
1500	300	40	3.7	0.034	0.990
500	100	40	3.7	0.010	0.959
500	200	40	3.7	0.018	0.994
500	400	40	3.7	0.094	0.998
500	300	20	3.7	0.025	0.990
500	300	60	3.7	0.143	0.972
500	300	40	3	0.522	0.950
500	300	40	7	0.048	0.949
500	300	40	9	0.024	0.960
500	300	40	11	0.005	0.954

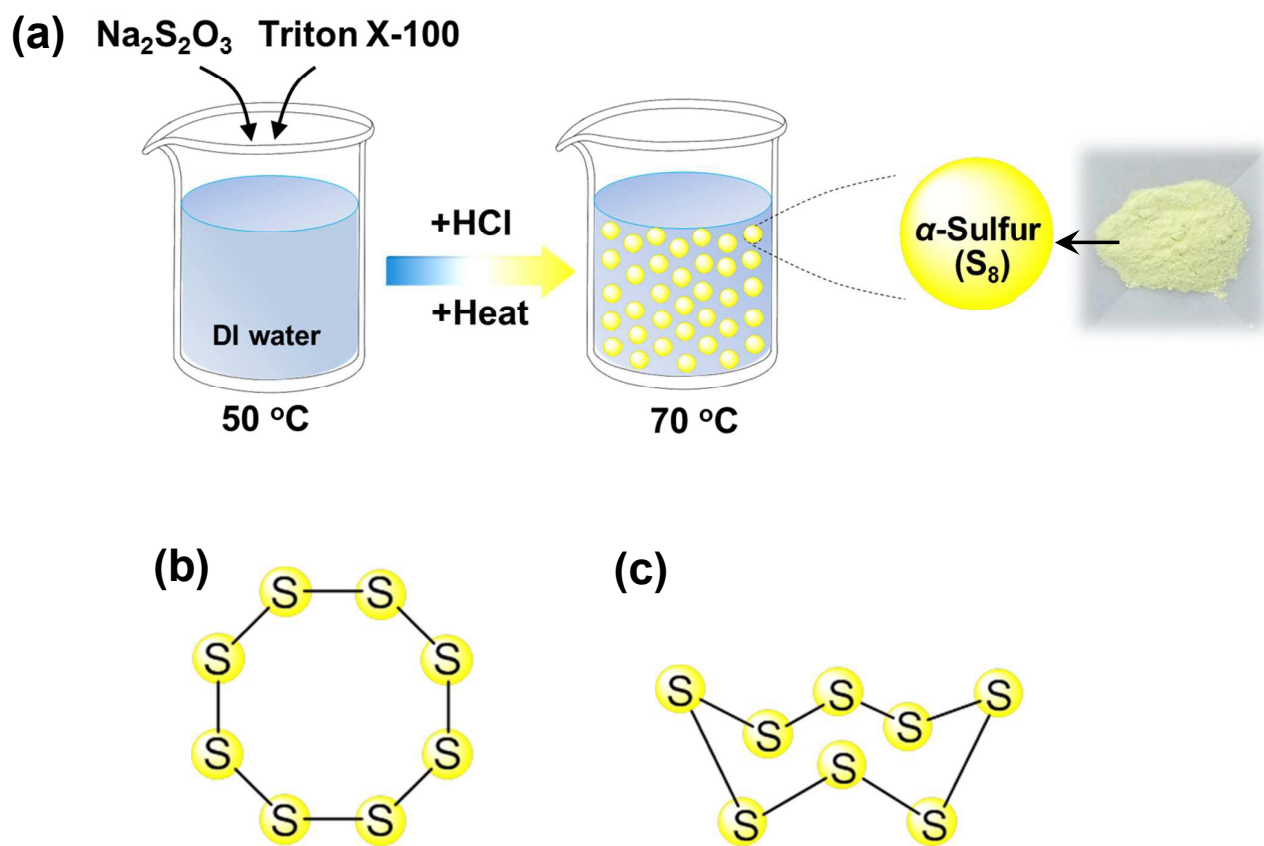


Fig. 1. The ring-structure  $\alpha$ -S: (a) preparation scheme, (b) top view and (c) side view of  $\alpha$ -S.

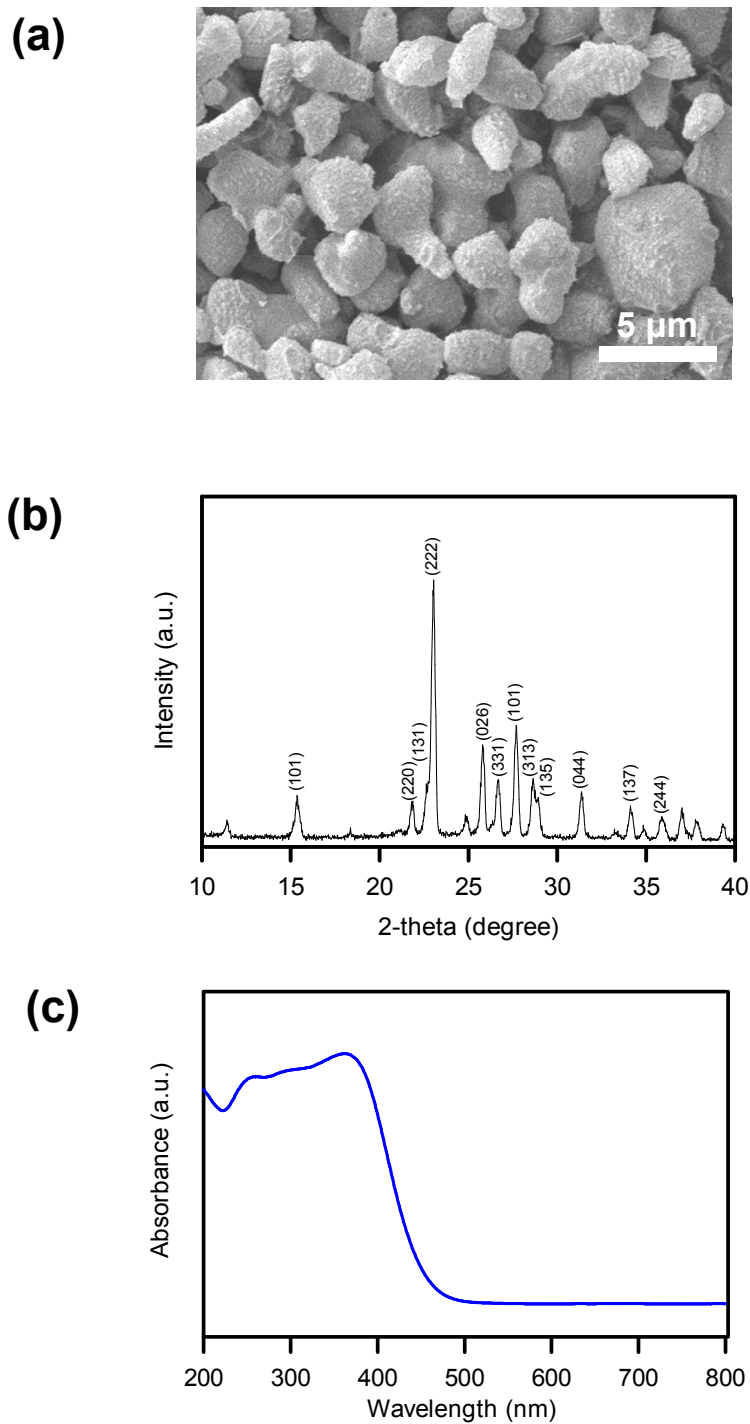


Fig. 2. Characteristics of  $\alpha$ -S: (a) SEM image, (b) XRD pattern and (c) DRS spectrum.

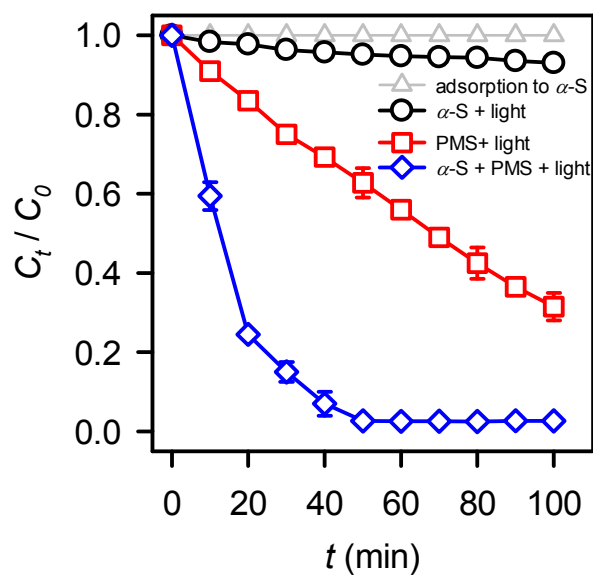


Fig. 3. Comparison of decolorization by adsorption to  $\alpha$ -S,  $\alpha$ -S under visible light irradiation ( $\alpha$ -S + light), PMS under visible light irradiation (PMS + light), and PMS activated using  $\alpha$ -S under visible light irradiation ( $\alpha$ -S + PMS + light) (PMS = 300 mg L<sup>-1</sup>,  $\alpha$ -S = 500 mg L<sup>-1</sup>, T = 40 °C;  $C_0$  of RhB = 10 mg L<sup>-1</sup>)

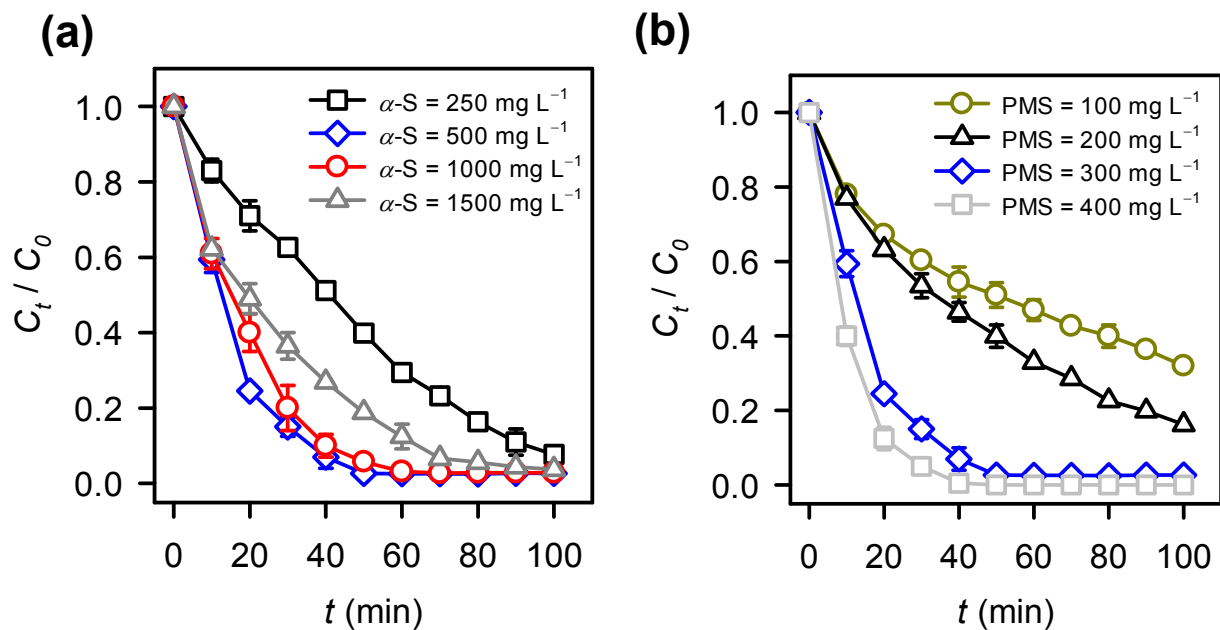


Fig. 4. Effects of (a)  $\alpha$ -S loading (PMS = 300 mg L<sup>-1</sup>, T = 40 °C), (b) PMS dosage ( $\alpha$ -S = 500 mg L<sup>-1</sup>, T = 40 °C) on the decolorization.  $C_0$  of RhB = 10 mg L<sup>-1</sup>.

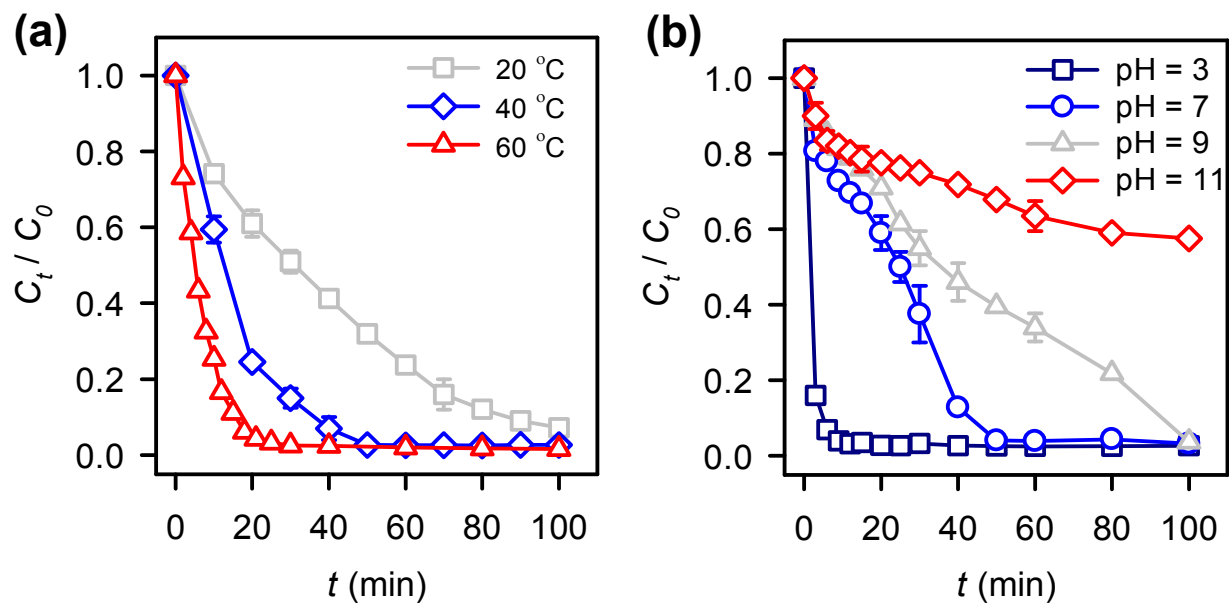


Fig. 5. Effects of (a) temperature and (b) pH on the decolorization. PMS = 300 mg  $L^{-1}$ ;  $\alpha$ -S = 500 mg  $L^{-1}$ ;  $C_0$  of RhB = 10 mg  $L^{-1}$ ; T = 40 °C;  $C_0$  of RhB = 10 mg  $L^{-1}$ .

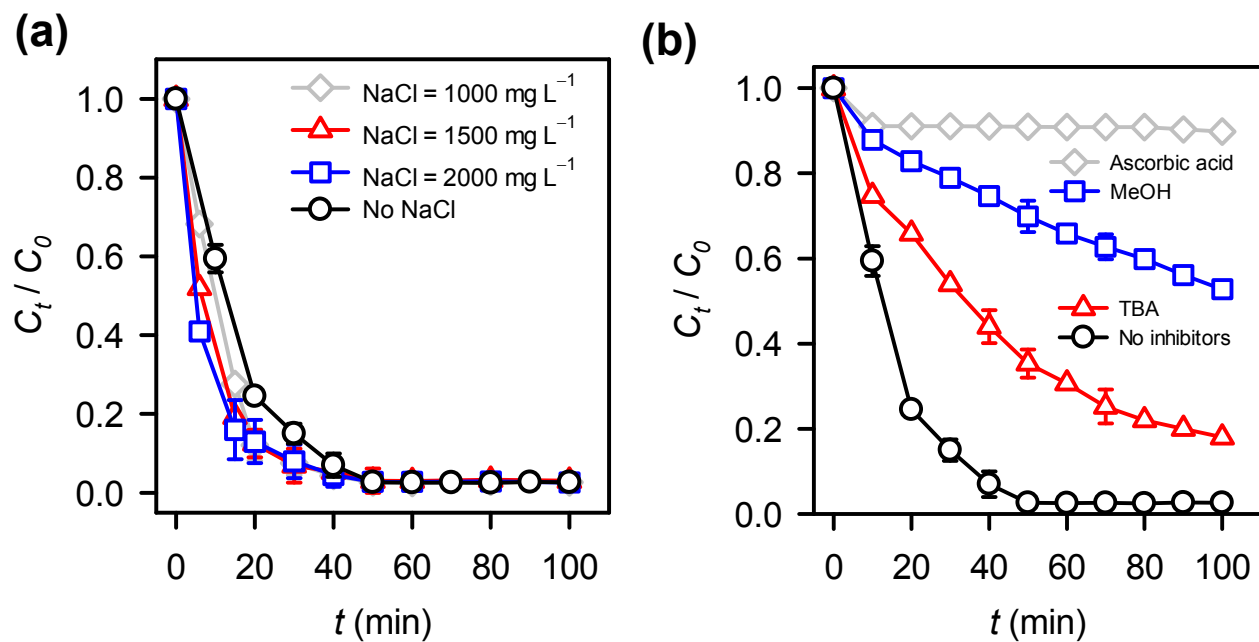


Fig. 6. Effects of (a) NaCl and (b) inhibitors (ascorbic acid = 0.01 M, methanol = 0.2 M and TBA = 0.2 M) on the decolorization. PMS = 300 mg L<sup>-1</sup>;  $\alpha$ -S = 500 mg L<sup>-1</sup>;  $C_0$  of RhB = 10 mg L<sup>-1</sup>; T = 40 °C.

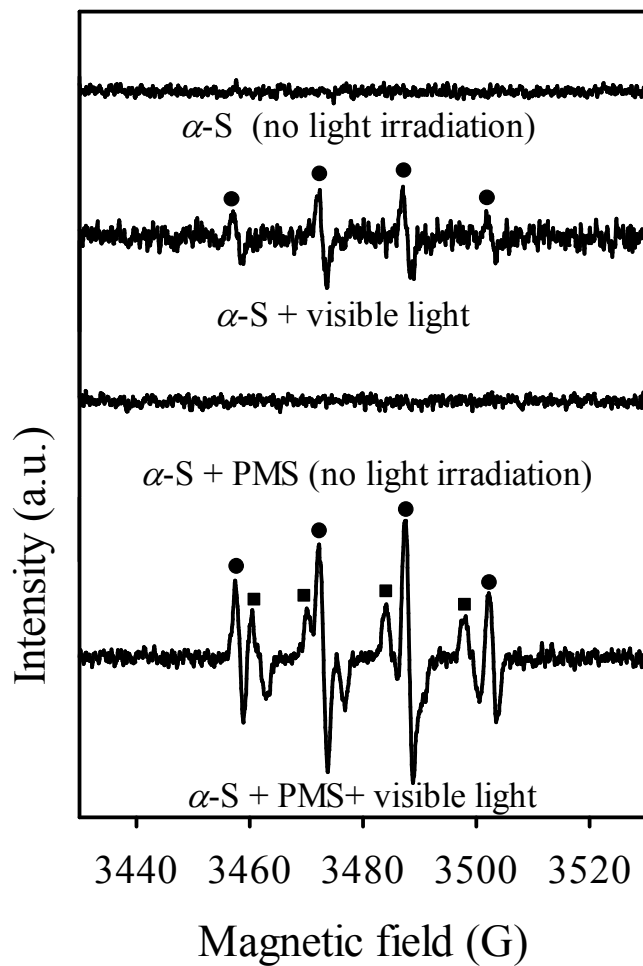


Fig. 7. Electron paramagnetic resonance (EPR) spectra of  $\alpha$ -S with and without visible light irradiation (■: DMPO-SO<sub>4</sub> and ●: DMPO-OH) (PMS = 300 mg L<sup>-1</sup>;  $\alpha$ -S = 500 mg L<sup>-1</sup>; DMPO = 500 mg L<sup>-1</sup>; T = 25 °C).

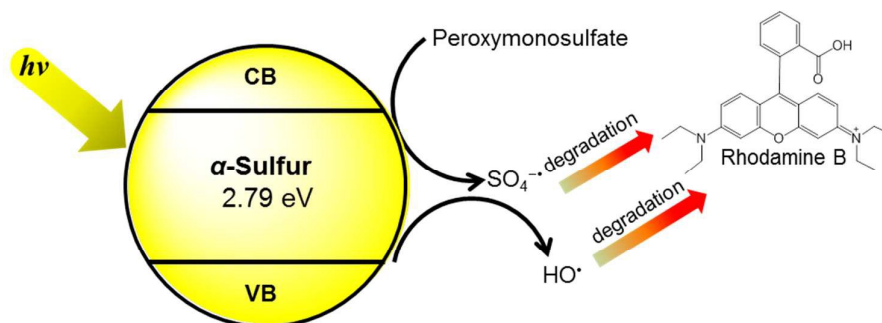


Fig. 8. A proposed mechanism of PMS activated by  $\alpha$ -S/Vis process for the decolorization.

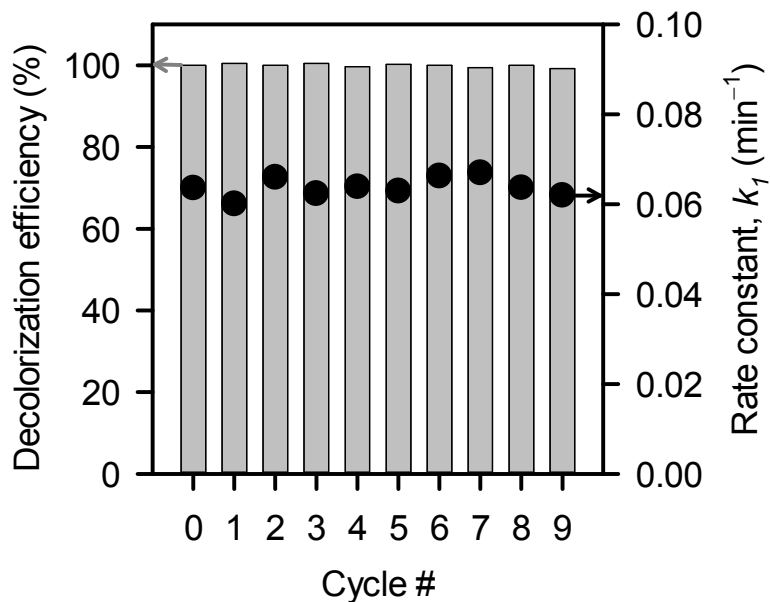


Fig. 9. Recyclability of  $\alpha$ -S/Vis to activate PMS for the RhB decolorization (PMS =  $300 \text{ mg L}^{-1}$ ;  $\alpha$ -S =  $500 \text{ mg L}^{-1}$ ;  $C_0$  of RhB =  $10 \text{ mg L}^{-1}$ ; T =  $40 \text{ }^\circ\text{C}$ ).

